The spatial distribution of magnetisation density in Mn_5Ge_3

1990 J. Phys.: Condens. Matter 2 2713

(http://iopscience.iop.org/0953-8984/2/11/014)

J. Phys.: Condens. Matter **2** (1990) 2713–2720. Printed in the UK

The spatial distribution of magnetisation density in Mn_5Ge_3

J B Forsyth† and P J Brown‡

† Neutron Science Division, Rutherford Appleton Laboratory, Chilton,
Oxon OX11 0QX, UK
‡ Institut Laue–Langevin, BP 156, 38042 Grenoble Cédex, France

Received 10 November 1989

Abstract. The spatial distribution of magnetisation density in the intermetallic compound Mn_5Ge_3 has been determined from a polarised neutron diffraction single-crystal study at 4.2 K. The positional and thermal parameters of the structure were derived from an unpolarised neutron study at 60 K, which also served to characterise the extinction in the material. The observed magnetic structure factors were fitted by a multipole expansion based on free-atom form factors for each of the two crystallographically inequivalent manganese atoms in the unit cell. The magnetic moment of the Mn1 atom with site symmetry 32 is 1.96(3) μ_B and that of Mn2 with site symmetry mm is 3.23(2) μ_B. The radial form factor of the Mn1 atom is found to be significantly contracted relative to that of a free Mn^{2+} ion. Evidence is presented that Mn–Mn interactions are the major factor leading to the difference in the moments on the two sites.

1. Introduction

The intermetallic compound Mn_5Ge_3 is ferromagnetic below its Curie temperature of 304 K (Tawara and Sato 1963), with a saturation magnetisation of 2.60(2) μ_B/Mn atom at 4.2 K (Kappel *et al* 1973). Its crystal structure is of the $D8_8$ type (space group $P6_3/mcm$) shown in figure 1, with cell dimensions at ambient temperature of $a = 7.184(2)$ and $c = 5.053(2)$ Å. This cell contains two crystallographically independent sets of manganese atoms: Mn1 in a four-fold position with 32 symmetry and Mn2 in a six-fold position with mm symmetry. Earlier polarised neutron diffraction measurements at 77 K by the present authors (Forsyth and Brown 1964) gave moment values of 1.7(1) and 2.7(1) μ_B for Mn1 and Mn2, in contradiction to a prediction by Kanematsu (1962), who proposed saturation values of 3 and 2 μ_B respectively. Further evidence to support our observation that the Mn2 site carries the larger moment was provided by the zero-field NMR measurements of Jackson *et al* (1965), who associated the mean hyperfine field of 399 kOe with Mn2 atoms, whereas the field at the Mn1 site is only 195 kOe.

More recently, studies of magnetisation by Kappel *et al* (1976) and NMR by Pannisod *et al* (1982) in the ternary isostructural compounds $Mn_5(Ge_{1-x}Si_x)_3$ have renewed interest in the nature of the chemical bonding and magnetic interactions between manganese and metalloid atoms. In this paper we report a more extensive polarised neutron determination of the spatial distribution of magnetisation in the binary phase

0953-8984/90/112713 + 08 $03.50

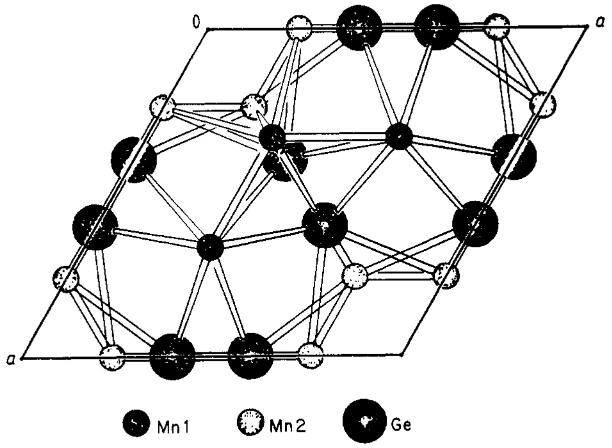

Figure 1. The structure of Mn_5Ge_3 viewed down [001].

Mn_5Ge_3, which we have undertaken as a preliminary to a study of ternary phases in the ferromagnetic regime which extends to $x = 0.8$.

2. Experimental details

All the single-crystal samples used in the diffraction experiments were cut with a diamond saw from a long rod prepared by the floating-zone technique from previously arc-melted superpure starting elements. Three pillars one of cross section 3.85×2.75 mm^2 and long axis parallel to [001] and the others of cross section 1.5×1.5 mm^2 and long axes [001] and [010] respectively were used for the polarised beam flipping ratio measurements carried out on the D3 diffractometer at the Institut Laue–Langevin, Grenoble. An approximately equi-axed specimen, subsequently cut from the 1.5×1.5 mm^2 [010] pillar, was used on the four-circle unpolarised beam diffractometer D9 to collect the integrated intensity data required to refine the low temperature structural and thermal parameters and to characterise any extinction in the samples. These data were measured at 0.523, 0.705 and 0.909 Å with the specimen at 60 K, making use of the enhanced intensity of short wavelength neutrons provided by the reactor hot source.

3. The nuclear structure at 60 K

The data sets taken at the three different wavelengths and comprising some 1000 measurements were first averaged over equivalents giving merging R-factors of 1.8, 1.1 and 1.64% for 0.523, 0.705 and 0.909 Å data respectively. The 266 averaged reflections were then refined together with three different, but nearly equal, scale factors and a single value of the mosaic spread to describe the extinction, which was low, using the formalism of Becker and Coppens (1974). The magnetic scattering of the ferromagnetic structure with moments parallel to [001] was modelled using a form factor derived from the 3d wavefunctions of Clementi and Roetti (1974) for the Mn^{2+} free ion. The final R-factor was 1.4% for a unit weighting scheme and unchanged for a weighted refinement in which the estimated standard deviations, σ, of reflections were derived from the agreement between the intensities of equivalents, rather than their counting statistics, and the weights used were $1/\sigma^2$. This latter refinement gave a χ^2 value of 6.4 and a weighted R-factor of 1.15% on structure factors. The parameters corresponding to this fit are:

Atom	Position	Parameter	ITF	μ_B
Mn1 in 4(d)	$(\frac{1}{3}\,\frac{2}{3}\,\frac{1}{4})$		0.13(1)	1.94(3)
Mn2 in 6(g)	$(x\,0\,\frac{1}{4})$	$x = 0.2397(1)$	0.20(1)	3.34(2)
Ge in 6(g)	$(x\,0\,\frac{1}{4})$	$x = 0.6030(1)$	0.14(1)	

The mosaic spread parameter was $0.098(10) \times 10^{-4}\ \mathrm{rad}^{-1}$ with the domain radius fixed at 100 μm.

4. The magnetisation density

Polarised beam flipping ratios were measured on the D3 diffractometer at the Institut Laue–Langevin, Grenoble. The diffractometer is fitted with a detector whose axis can be tilted out of the horizontal plane by angles of up to about 25° to allow reflections, whose scattering vectors are not in this plane, to be measured in normal-beam geometry. The majority of the measurements were made on the two [001] pillars, since this is the easy direction of magnetisation in the material (Tawara and Sato 1963) and saturation could be achieved at 4.2 K in the 1.5 T field of the available electromagnet. Measurements of the flipping ratios of all reflections with $\sin\Theta/\lambda < 0.8$ Å^{-1} in the zero, first and second layers were made at 0.924 Å on the larger pillar. Subsequently to test the validity of the extinction correction and to check for multiple scattering all reflections whose nuclear structure factors were greater than 0.2×10^{-12} cm were re-measured with wavelengths of 0.924 and 1.085 Å from the 1.5 × 1.5 mm cross-section pillar. A short period of time was also available with a superconducting magnet system giving a maximum field of 4.6 T which enabled us to saturate the [010] axis pillar parallel to its long axis and measure reflections in the zero, first and second layers up to the same $\sin\Theta/\lambda$ limit at a wavelength of 0.924 Å. To investigate a possible difference in the magnetic anisotropy of the two manganese sites a set of 65 flipping ratios of *h*0*l* reflections was also measured at a lower field of 1 T.

The observed flipping ratios were corrected for the small degree of extinction using the parameter found from the D9 experiment and for the lack of perfect polarisation and spin flipping. The values of γ, the ratio of magnetic to nuclear structure factor, were then averaged for each group of equivalent reflections and the magnetic structure factor obtained by multiplying γ by the corresponding nuclear structure factor calculated from our refined model. In most cases, the data for equivalent reflections were in good agreement, irrespective of the specimen or wavelength involved. Some significant discrepancies did occur with certain, generally weak reflections and these were attributed to the effects of multiple scattering. Omitting these dubious data and carrying out a least-squares refinement for the two manganese moments using a form factor derived from the free atom 3d wavefunctions of Clementi and Roetti (1974) led to an R-factor of 10.4% and moments of 1.85(3) and 3.23(3) μ_B for Mn1 and Mn2 respectively. At this stage, the χ^2 value was 32 and the weighted R-factor 9.6%. A similar treatment of the data measured at 1 T gave moment values each of which was reduced by a factor of 0.80 from the saturated value: so we conclude that the anisotropies of the two sites are the same.

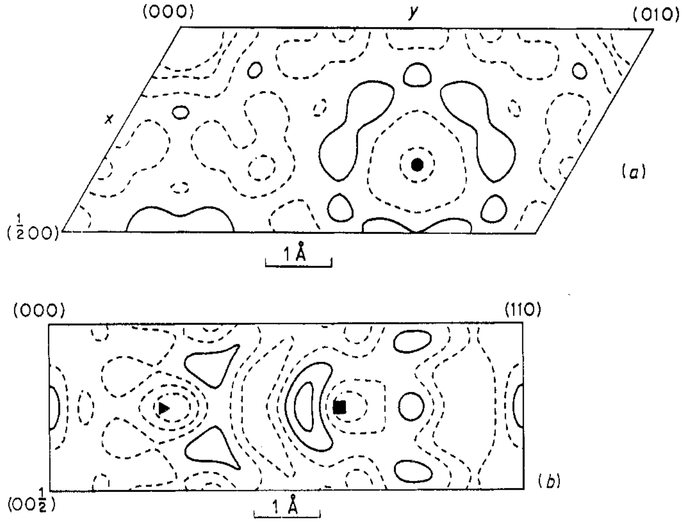

Figure 2. Difference Fourier sections through the Mn sites. (*a*) perpendicular to [001] through Mn1 (full circle) and (*b*) perpendicular to [1$\bar{1}$0] through Mn (full triangle) and Ge (full square). The contour intervals are 0.13 μ_B Å^{-3}, negative contours are shown by broken contours. The figures in parentheses are the coordinates of the map position on the crystallographic axes.

The possibility that the true form factors might have a different radial dependence than that corresponding to the free ion was then allowed for by refining a contribution to the radial form factor for each atom with the angular dependence of the associated $\langle j_2 \rangle$ radial integral (Watson and Freeman 1961). A small, but significant negative coefficient was found for the Mn1 atom, corresponding to a contraction of the form factor indicating an expansion in the magnetisation density, and this lowered the *R*-factor to 8.5% and χ^2 to 29. The model was then extended to include multipole functions, with 3d radial distributions and symmetries appropriate to that of the Mn1 (32) and Mn2 (mm) sites. The least-squares fit of the occupation parameters of all allowed even multipoles up to $l = 4$ gave an *R* of 5.7%, but the amplitudes of a number of them were not significant. These amplitudes were then set at zero and the refinement repeated: table 1 lists the final amplitudes and the local axes on which the multipoles are described. The moment values corresponding to this improved fit are 1.96(3) and 3.23(2) μ_B with an *R*-factor of 5.8%. The total localised moment per cell is 27.2(2) μ_B, slightly higher than the 26.0(2) μ_B given by the saturation magnetisation measurements of Kappel *et al* (1973). There is therefore some evidence for the existence of spatially diffuse reverse magnetisation in Mn_5Ge_3 amounting to some 0.1 μ_B/Mn, such as has been found in the ferromagnetic transition elements.

The χ^2-value of 12 suggests that our multipole model is less than perfect and that the data contain further significant information. Although it is clear that most of the magnetisation is centred on the manganese atoms, the possibility that there is some which is associated with p orbitals on the germanium was investigated: no significant improvement was obtained by including multipole functions with $l = 0$ and 2 having Ge 3p radial distributions. Figure 2 shows the difference Fourier sections through the Mn sites which correspond to the model of table 1: (*a*) perpendicular to [001] through Mn1

Table 1. Final refined values for the significant multipoles describing the magnetisation density in Mn_5Ge_3.

	Atom Mn1		Atom Mn2		
	Y00	1.96(3)		Y00	3.23(2)
	Y40	−0.17(5)		Y20	0.08(2)
				Y22+	0.13(2)
	$\langle j_2 \rangle$	−0.05(2)			
Local axes:	x parallel to a^*		Local axes:	x parallel to [001]	
	z parallel to [001]			$z$parallel to [100]	

and (*b*) perpendicular to $[1\bar{1}0]$ through Mn2 and Ge. There are significant features in these maps associated with all three atomic sites: both manganese sites are found in regions of negative density which must be more diffuse than that corresponding to the 3d form factors of the fit. The form of the density at the germanium site seen in figure 2(*b*) is highly asymmetric, which explains why it was not possible to model it with even multipoles. The atom centre is again in a region of negative density and a significant positive lobe lies close to it on the side of the Mn2 neighbour on the same diad axis.

5. Discussion

Thanks to magnetisation and neutron diffraction measurements there is now a considerable body of data available on the variation of magnitudes of ordered transition metal moments brought about by alloying with B-subgroup metals. Very generally such alloying is found to reduce the moments from the values characteristic of the ions. Such reduction, similar to that which occurs in the pure elements, is attributed to participation of the d electrons in the Fermi surface. There is as yet however no general understanding of the way in which either transition-metal–metalloid (T–M) or inter-transition-metal (T–T) interactions modify the transition metal d bands and hence the magnetic moments. Within a semi-rigid band model, the moment variations in transition-metal–metalloid (T–M) alloys at low M concentrations may be attributed to transfer of electrons from the sp band of the M atom to the T atom d band. However, Mössbauer measurements by Bernas *et al* (1967) and by Takács *et al* (1975) on Fe–M alloys have shown that the isomer shift, which is sensitive to the 3d density near the iron nucleus, is constant regardless of metalloid type and concentration. Alternatively it has been proposed by Takács *et al* (1975) and by Alben *et al* (1978) that changes in band structure due to bonding between T and M atoms are responsible for the moment reduction with increasing M content. Following this approach Corb *et al* (1982a) have described a model which accounts quantitatively for the moment variations in T–M crystals and glasses in which T = Co or Fe at M concentrations up to 30%.

The local environment of the Mn atoms in Mn_5Ge_3 are given in table 2 and illustrated in figure 3. Mn1 has six Ge, six Mn2 and two Mn1 neighbours whereas Mn2 has five Ge, four Mn1 and six Mn2 neighbours. Within the bond model of Corb, the rather small change in Ge coordination seems inadequate to explain the large difference between the moments of Mn1 and Mn2. On the other hand, although Mn1 has only eight Mn neighbours as opposed to the ten Mn neighbours of Mn2, two of the former group are

Table 2. Interactomic distances (Å) to the atoms coordinating Mn1 and Mn2 atoms in Mn_5Ge_3.

Mn1 to	2 × Mn1 at 2.522	Mn2 to	2 × Mn2 at 2.976
	6 × Mn2 at 3.059		4 × Mn2 at 3.051
			4 × Mn1 at 3.059
	6 × Ge at 2.534		2 × Ge at 2.482
			1 × Ge at 2.606
			2 × Ge at 2.762

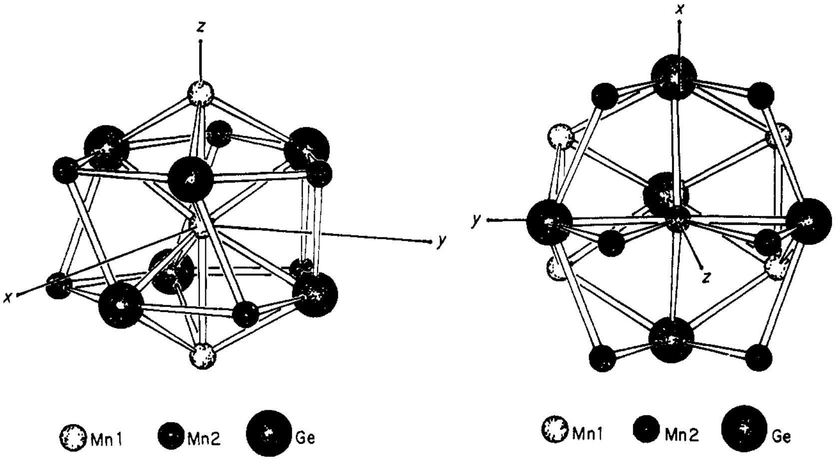

Figure 3. The coordination of the Mn1 and Mn2 atoms viewed a 5° to [110]. The local axes chosen for the multipole model of the magnetisation density are also shown.

at the very short distance of 2.522 Å. This suggests that it may be Mn–Mn interactions which are responsible for the low moment observed for Mn1. With this in mind we have explored the possibility that changes in the coordination of manganese by manganese are responsible for the wide range of ordered moment values in Mn–M intermetallics. It is known that even in metallic systems Mn atoms can exhibit moments approaching the 5 μ_B of the Mn^{2+} ion. This occurs in systems such as the Heusler alloys where the Mn atoms are well separated from each other (Webster and Tebble 1967). If we assume that below some critical interatomic distance Mn atom neighbours reduce the moment of the coordinated Mn atom from the ionic value, and that this moment reduction increases linearly with decreasing interatomic separation, there should be a linear relationship between the moment reduction per coordinating atom ($\Delta\mu$) and the mean coordination distance Λ. In figure 4 $\Lambda\mu$ is plotted against Λ for the ferromagnetic Mn–metalloid compounds Mn_5Ge_3, $Mn_{1.09}Sb$ (Reimers *et al* 1983), Mn_2Sb (Alperin *et al* 1963), MnSi (Brown *et al* 1968, Levinson *et al* 1973) and MnP (Forsyth *et al* 1966), which cover a range of Mn moments from 0.4 to 3.45 μ_B. These data suggest that the threshold separation is some 3.1 Å and that below this distance the moment reduction is $\simeq 2\ \mu_B\ Å^{-1}$. The data for α-manganese itself (Yamada *et al* 1970) are also plotted in figure 4: there is a similar linear relationship but the moment reduction per Å is reduced to 0.9 $\mu_B\ Å^{-1}$ and the threshold separation lowered to 2.95 Å. It therefore appears that the presence

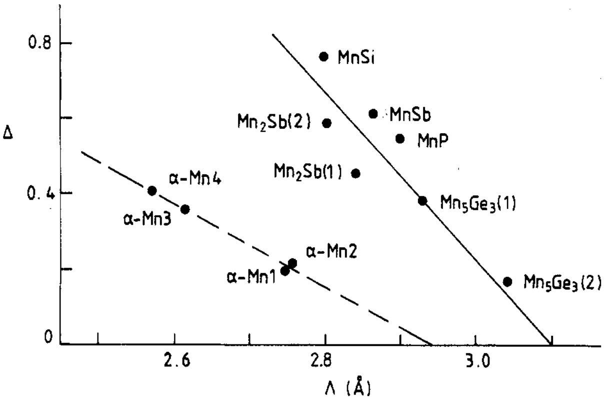

Figure 4. The moment reduction from $5\mu_B$ per Mn ligand (Δ in μ_B) of Mn atoms in some ferromagnetic Mn–metalloid intermetallic compounds plotted against the mean Mn–Mn bond length (Λ). The approximately linear arrangement of the data and the intecept at 3.1 Å on the Λ axis suggests that Mn–Mn interactions at less than this distance lead to moment reductions of about $2\,\mu_B$ Å^{-1}/bond. The lower line of points correspond to data for α-Mn and show a lower slope and a smaller critical distance.

of metalloid atoms reduces the stability of manganese moments to the effects of Mn–Mn interactions.

As far as the radial extent of the magnetisation is concerned, that of the Mn2 atom has a form similar to that of a free Mn^{2+} ion, but there is evidence for a small expansion of the density around the low moment Mn1 atoms. A similar expansion was also noted by Alperin *et al* (1963) for the low moment site in Mn_2Sb. Looking at the departures from spherical symmetry: the only significant higher multipole which could be fitted to the Mn1 density was Y40 with a normalised amplitude of -0.1. This negative coefficient indicates a contraction of the magnetisation both along [001], the direction of its two closest Mn neighbours, and in the (001) plane. The density is correspondingly extended towards the six germanium ligands. The lower symmetry of the Mn2 site is reflected in the occurrence of significant $l = 2$ multipoles, whereas none of the significance were found for $l = 4$. The amplitudes determined for Y20 and Y22 again describe magnetisation extended in the direction of the Ge ligands. It is reasonable to associate the residual acentric density near Ge with its asymmetric coordination by Mn2. The positive lune of density around Ge is the only significant positive region in the difference map and is probably due to hybridisation between Mn 3d and Ge sp states. The predominance of reverse magnetisation elsewhere in the cell is characteristic of metal–metal bonding in 3d transition metals (Moon 1982).

References

Alben R A, Budnick J I and Cargill G S III 1978 *Metallic Glasses* ed J J Gilman and H J Leamy (Cleveland, OH: American Society for Metals) p 304

Alperin H A, Brown P J and Nathans R 1963 *J. Appl. Phys.* **34** 1201

Becker P and Coppens P 1974 *Acta Crystallogr.* A **30** 129

Bernas H, Campbell I A and Fruchart R 1967 *J. Appl. Phys. Chem. Solids* **28** 17

Brown P J, Forsyth J B and Lander G H 1968 *J. Appl. Phys.* **39** 1331

Clementi E and Roetti C 1974 *At. Data Nucl. Data Tables* **14** 177

Corb B W, O'Handley R C and Grant N J 1982a *J. Appl. Phys.* **53** 7728

Forsyth J B and Brown P J 1964 *Proc. Int. Magnetism Conf. (Nottingham)* (London: The Physical Society) p 524

Forsyth J B, Pickart S J and Brown P J 1966 *Proc. Phys. Soc.* **88** 333

Jackson R F, Scurlock R G, Utton D B and Wray E M 1965 *Proc. Phys. Soc.* **85** 127

Kanematsu K 1962 *J. Phys. Soc. Japan* **17** 85

Kappel G, Fischer G and Jaéglé A 1973 *Phys. Lett.* **45A** 267

—— 1976 *Phys. Status Solidi* **34** 691

Levinson L M, Lander G H and Steinitz M O 1973 *Magnetism and Magnetic Materials (Denver, CO, 1972)* (New York: American Institute of Physics)

Moon R M 1982 *J. Physique Coll.* **43** C7

Panissod P, Qachaou A and Kappel G 1982 *Proc. Int. Magnetism Conf. (Kyoto)* (Amsterdam: North-Holland) pp 701

Reimers W, Hellner E, Treutmann W and Brown P J 1983 *J. Phys. Chem. Solids* **44** 195

Takács L, Cadeville M C and Vincze I 1975 *J. Phys. F: Met. Phys.* **5** 800

Tawara Y and Sato K 1963 *Proc. Phys. Soc. Japan* **18** 773

Watson R E and Freeman A J 1961 *Acta Crystallogr.* **14** 27

Webster P J and Tebble R S 1967 *Phil. Mag.* **16** 347

Yamada T, Kunitomi N, Nakai Y, Cox D and Shirane G 1970 *J. Phys. Soc. Japan* **28** 615